Removal of Dispersion Penalty of Time-Stretch Photonic Analog-to-digital Conversion System by Use of Chirped Intensity Modulator

Hongnan Li, Weiwen Zou,* and Jianping Chen
State Key Lab of Advanced Optical Communication Systems and Networks,
Department of Electronic Engineering, Shanghai Jiao Tong University, Shanghai 200240, China
**Corresponding author: wzou@sjtu.edu.cn*

Abstract: A novel scheme using dual-output Z-cut intensity modulator with fixed chirp is demonstrated to remove dispersion penalty of time-stretch photonic analog-to-digital conversion system. A modified algorithm is presented to effectively recover the distorted signal.
OCIS codes: (070.1170) Analog optical signal processing; (260.2030) Dispersion; (320.1590) Chirping

1. Introduction

Time-stretch photonic analog-to-digital conversion (TS-PADC) system has been developed rapidly during the past decades since it can boost the performance (such as sampling rate) of electric ADC by stretching the signal in time domain and compressing it in frequency domain for potential applications to modern radar, fiber-optic communications, ultrafast image capturing [1-3]. Dispersion is a key parameter for time-stretch in this system. However, its related effect, called dispersion penalty, is the key factor limiting the bandwidth of the TS-PADC system [4]. There are two basic methods to overcome or remove the dispersion penalty by employing proper modulators: single side band (SSB) modulator [5] or dual-output single-electrode Mach-Zehnder modulator (MZM) [4]. The SSB modulator has the limited bandwidth of ~20 GHz due to the electric components; while the later can provide much broader bandwidth. Its removal of dispersion penalty is attributed to the chirp factor of -1, which makes the dual outputs complementary in phase [4]. Z-cut push-pull intensity MZM with a fixed chirp factor is commercially mature for optical-fiber telecom. In [6], this Z-cut MZM was modeled as a single electrode MZM and its chirp factor wasn't considered for analyzing analog optical links.

In this work, the impact of the chirp factor of the Z-cut push-pull intensity MZM on the TS-PADC system is investigated. It is found that the chirp factor plays an important role in the dual complementary outputs of the Z-cut MZM. A modified algorithm with considering the chirp factor is presented to effectively remove dispersion penalty.

2. Principle and results

The basic structure of a push-pull dual-output Z-cut intensity MZM is illustrated in Fig. 1(a). When a voltage of *V* is applied, a positive phase shift $\varphi_1(V)$ is induced in the one arm and a negative phase shift $\varphi_2(V)$ is induced in the other. The chirp factor α is defined by [7]:

$$\alpha = \frac{\varphi_2 + \varphi_1}{\varphi_2 - \varphi_1} \tag{1}$$

where $|\varphi_1| \neq |\varphi_2|$ for a Z-cut push-pull intensity MZM [8] different from zero-chirp push-pull MZM.

Suppose the electric field of the input optical pulse is $E_{in}(t)$, the electric field of the dual outputs can be represented as:

$$\begin{aligned} E_{out,1} &= \frac{E_{in}(\mathrm{t})}{2}\left(\mathrm{e}^{j\frac{\varphi_1}{\varphi_1-\varphi_2}(\frac{\pi}{2}+\mathrm{m}\cos(2\pi\,\mathrm{ft}))} - \mathrm{e}^{j\frac{\varphi_2}{\varphi_1-\varphi_2}(\frac{\pi}{2}+\mathrm{m}\cos(2\pi\,\mathrm{ft}))}\right) \\ E_{\mathrm{out},2} &= \frac{jE_{in}(\mathrm{t})}{2}\left(\mathrm{e}^{j\frac{\varphi_1}{\varphi_1-\varphi_2}(\frac{\pi}{2}+\mathrm{m}\cos(2\pi\,\mathrm{ft}))} + \mathrm{e}^{j\frac{\varphi_2}{\varphi_1-\varphi_2}(\frac{\pi}{2}+\mathrm{m}\cos(2\pi\,\mathrm{ft}))}\right) \end{aligned} \tag{2}$$

where *m* is the modulation index and $cos(2\pi ft)$ is the modulated RF signal with *f* the signal frequency in GHz. Note that the Z-cut MZM is assumed to be biased at the quadrature point.

Figure 1(b) depicts the experimental setup of our configured TS-PADC system based on a $LiNbO_3$ Z-cut push-pull MZM (EOSPACE, 40-GHz bandwidth). A passively mode-locked fiber laser at 37-MHz repetition rate, sliced by an optical bandpass filter, serves as an optical pulse train source with 3.5-nm bandwidth centered at 1550 nm. The pulse train propagates through a spool of DCF with the total dispersion of -360 ps/nm, creating a chirped pulse with a time aperture of ~1.2 ns. After amplified by the erbium-doped fiber amplifier (EDFA), the dual outputs of the Z-cut MZM are simultaneously modulated by the same RF sinusoidal signal (see Eq. (2)). They are time-interleaved by a 3-dB 2×2 coupler after one is delayed by a half of the repetition period of the pulse train (= 13.5 ns). The time stretch of the two time-interleaved signals is simultaneously performed when they propagate through the second spool of DCF with the total dispersion of -2519 ps/nm. The stretch factor is estimated to be M = ~8.1. Another EDFA is inserted in front of a photo-detector (PD) in order to achieve better signal-to-noise ratio (SNR) during the digitalization. The signal is finally captured by a real time oscilloscope with a sampling rate of 25 GS/s, which denotes the sampling rate of the TS-ADC equal to 203 GS/s.

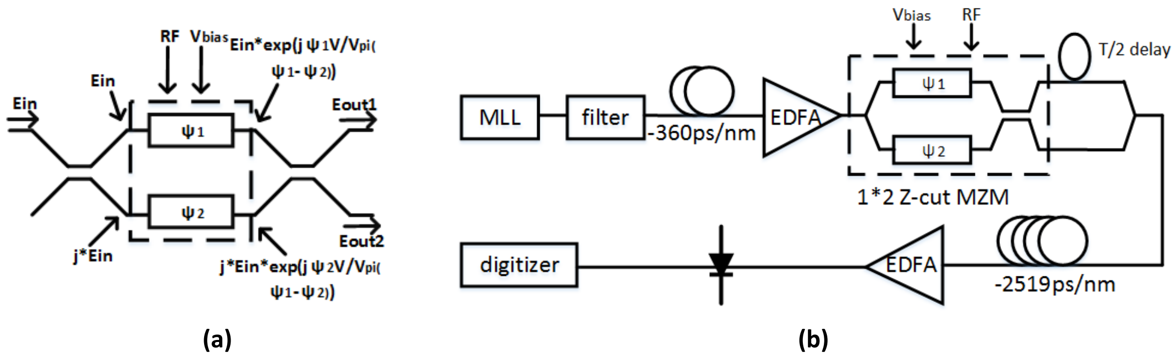

Fig. 1. (a) Basic structure of dual outputs Z-cut intensity modulator and (b) Experimental setup of the proposed TS-PADC by use of this modulator.

The RF power spectra (I_1 and I_2) of the dual outputs of the TS-PADC system are determined by their responses (H_1 and H_2) as $I_1 = \sqrt{2} m H_1 \cos(\frac{2\pi ft}{M})$ and $I_2 = \sqrt{2} m H_2 \cos(\frac{2\pi ft}{M})$, respectively. The two responses are defined by:

$$H_1 = -\sqrt{\frac{1+\alpha^2}{2}}\cos(\phi_{DIP} + \frac{\pi}{4} + \mathrm{arctg}\frac{\alpha+1}{\alpha-1})$$
$$H_2 = \sqrt{\frac{1+\alpha^2}{2}}\cos(\phi_{DIP} - \frac{\pi}{4} - \mathrm{arctg}\frac{\alpha+1}{\alpha-1}) \quad (3)$$

where $\phi_{DIP} = 2\pi^2 \beta_2 L_2 f^2 / \mathrm{M}$ is the dispersion induced phase in the TS-PADC system [4], β_2 is the second-order group-velocity dispersion, and L_2 is the length of the second spool of dispersion compensating fiber (DCF). It shows that the chirp factor plays an important role in the dispersion penalty of the TS-PADC system.

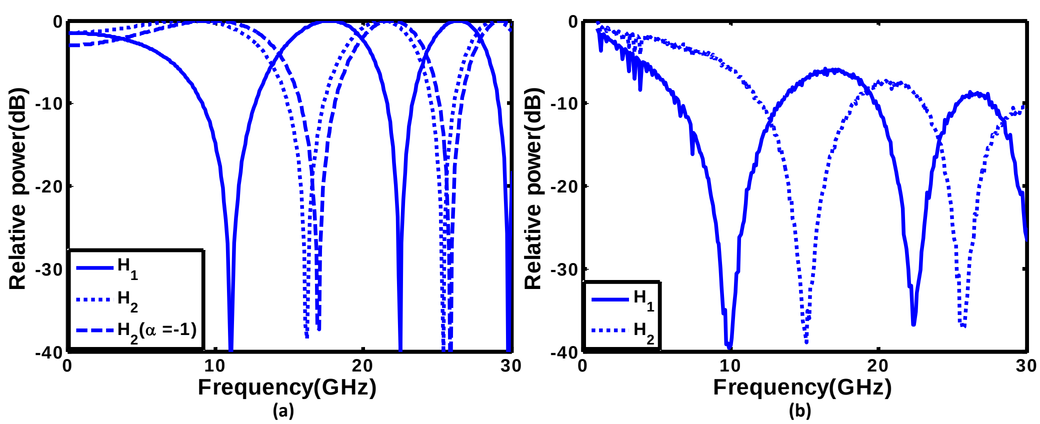

Fig. 2. Simulated (a) and measured (b) dispersion penalty of the dual outputs Z-cut modulator. Single-electrode MZM is also include in (a) for clear comparison.

Figure 2 illustrates a comparison of the simulated and measured dispersion penalty of the TS-PADC system. The simulation (see Fig. 2(a)) is implemented based on Eq. (3) and the parameters are set as follows: φ_{DIP} is set to be $8.2\times10^{-3} f^2$ and α is set to be -0.64. Compared with the case of a dual-output single electrode MZM with $\alpha = -1$ [4], it is clear that the dual outputs become not perfectly complementary due to the chirp factor. The measured dispersion penalty curves are plotted in Fig. 2(b). It is worth noting that the power attenuation in Fig. 2(b) is mainly caused by the RF response of the MZM and PD.

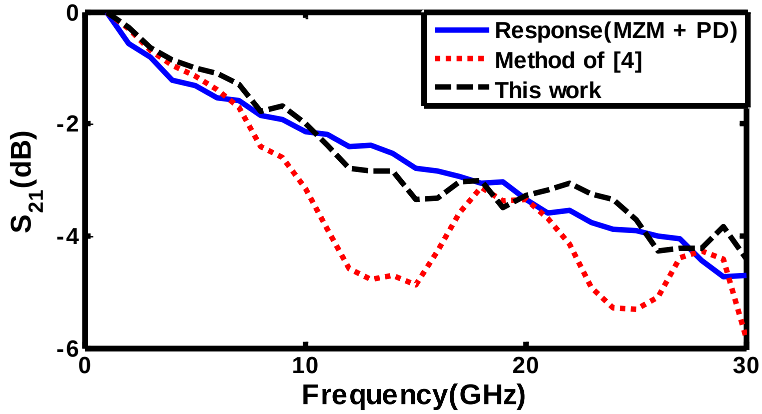

Fig. 3. Comparison between the ideal response of the MZM and PD and the recovered signal of the TS-PADC system based on the modified or original algorithm.

In despite of the imperfectly complementary feature, the dual outputs can be also utilized to effectively remove the dispersion penalty because when the signal power of one output decays to zero, that of the other still stays at a high value. However, taken into account the chirp factor, the algorithm proposed in [4] no longer behaves as expected, and a modified algorithm is proposed here to recover the modulated RF signal *I*, as follows:

$$I = \frac{(I_1 - I_2)\cos(\phi_{DIP})}{2\cos(\frac{\pi}{4} + arctg\frac{\alpha+1}{\alpha-1})} - \frac{(I_1 + I_2)\sin(\phi_{DIP})}{2\sin(\frac{\pi}{4} + arctg\frac{\alpha+1}{\alpha-1})} \quad (4)$$

The value of φ_{DIP} of the TS-PADC and the chirp factor of the MZM are first estimated based on the minimum mean square error (MMSE). Later, the RF response (S_{21} curve) of the TS-PADC is recovered based on Eq. 4, as plotted in Fig. 3 (see dashed curve). The response of the Z-cut MZM and PD, which is directly measured by use of a vector network analyzer (VNA, Agilent PNA-X Network analyzer N5247A), is also compared in Fig. 3 (see solid curve). The proposed scheme of the TS-PADC based on the Z-cut modulator with a fixed non-zero chirp factor and the modified algorithm clearly identifies the ideal response. However, the original algorithm [4] omitting the chirp factor (see dotted curve in Fig. 3) deviates seriously from the ideal response.

4. Conclusions

We have demonstrated a TS-PADC by use of a dual-output Z-cut push-pull intensity MZM. The impact of the chirp factor of the MZM on the TS-PADC is theoretically and experimentally investigated. The recovered response based on the modified algorithm matches well with the ideal one.

Acknowledgments

This work was supported in part by the National Natural Science Foundation of China (61127016), and the State Key Lab Project of Shanghai Jiao Tong University (2014ZZ03016).

References

[1] K. Goda, K. K. Tsia, and B. Jalali, "Serial time-encoded amplified imaging for real-time observation of fast dynamic phenomena," *Nature*, 458(7242): 1145-1149 (2009).

[2] A. Fard, J. Y. Yang, B. Buckley, et al., "Time-stretch oscilloscope with dual-channel differential detection front end for monitoring of 100 Gb/s return-to-zero differential quadrature phase-shift keying data," *Optics Letters*, 36(19): 3804-3806(2011).

[3] A. Fard, S. Gupta, and B. Jalali, "Photonic time-stretch digitizer and its extension to real-time spectroscopy and imaging," *Laser & Photonics Reviews*, 7(2): 207-263(2013).

[4] Y. Han, O. Boyraz, and B. Jalali, "Ultrawide-band photonic time-stretch A/D converter employing phase diversity," *IEEE Transactions on Microwave Theory and Techniques*, 53(4): 1404-1408(2005).

[5] J. M. Fuster, D. Novak, A. Nirmalathas, et al., "Single-sideband modulation in photonic time-stretch analogue-to-digital conversion," *Electronics Letters*, 37(1): 67-68(2001).

[6] S. Gupta, O. Boyraz, and B. Jalali, "Dispersion penalty mitigation using polarization mode multiplexing in phase diverse analog optical links," *Optical Fiber Communication Conference*, OSA Technical Digest, San Diego, California, USA, paper JThA76, 2008.

[7] T. Kawanishi, K. Kogo, S. Oikawa, et al., "Direct measurement of chirp parameters of high-speed Mach–Zehnder-type optical modulators," *Optics communications*, 195(5): 399-404(2005).

[8] E. L. Wooten, K. M. Kissa, A. Yi-Yan, et al., "A review of lithium niobate modulators for fiber-optic communications systems," *IEEE Journal of Selected Topics in Quantum Electronics*, 6(1): 69-82(2000).